

Low-Frequency Power Telemetry Using Multiferroic Laminate Heterostructures

Veeru Jaiswal*
Biomedical Engineering
Florida International University
Miami, USA
vjais001@fiu.edu

Pawan Gaire
Department of Electrical and Computer
Engineering, University of Nebraska-
Lincoln,
NE, USA,
pgaie2@huskers.unl.edu

Shubhendu Bhardwaj
Department of Electrical and Computer
Engineering, University of Nebraska-
Lincoln,
NE, USA,
bhardwaj@unl.edu

Akeeb Yunus Hassan
Biomedical Engineering
Florida International University
Miami, USA
ahass05@fiu.edu

John L. Volakis
Department of Electrical and Computer
Engineering,
Florida International University
Miami, USA
jvolakis@fiu.edu

Pulugurtha Markondeya Raj
Biomedical Engineering
Florida International University
Miami, USA
mpulugur@fiu.edu

Abstract— Wireless power transmission is becoming a key technology in realizing future sensor nodes. Current approaches are based on inductive links or RF telemetry, both face limitations in achieving higher power densities. Multiferroic telemetry can address this challenge and provide a new approach for remote powering. This paper describes an integrated piezoelectric film on magnetostrictive carriers to achieve highly-efficient multiferroic functions. Various multi-layered architectures were investigated for output power performance. The multiferroic flexible stacks subsequently integrated with diode rectifier topologies and storage capacitors to generate the desired output. Results demonstrate new power telemetry opportunities with advanced material stacks with flex package integration.

Keywords— Piezoelectric; magnetostrictive, multiferroic; magneto-electric coupling, Power telemetry.

I. INTRODUCTION

Embedded power modules with planar and flexible packaging will eventually replace today's bulky modules using pre-packaged and discretely-mounted components on flex. We seek to advance package integration architectures and manufacturing paths to realize such future embedded power systems. Several technical challenges need to be addressed to realize power and data transfer within tiny nodes. A major challenge is to deliver power to sub-mm grains with adequate power transfer efficiency. Inductive coupling or RF power telemetry face fundamental challenges in meeting this goal. Our strategy is to achieve this goal through piezo-magnetostrictive coupling of external magnetic fields in bulk acoustic resonance modes to achieve high magnetoelectric coefficients. The objective of this research is to develop such integrated piezo-magnetostrictive architectures with rectifier and storage capacitors for next-generation high-efficiency remotely powered communication and sensing nodes. Under resonant conditions, we will show that such transducers can achieve the target power densities to drive sensing-signal and processing by leveraging wireless communication devices with minimal footprint. This technology will enable power delivery to all wearable, textile-embedded, or object-embedded electronic sensing and communication systems of the future. Further, the low-cost manufacturing path will enable high-volume production of power modules, bringing the best combination of wireless power or harvesting schemes

with rectification and storage. Modularity will also allow for ease in incorporating next-generation building-block components.

The discovery of a new class of multiferroic materials has led to the development of devices with improved performance, a result of strong magnetoelectric (ME) coupling. In such systems, both magnetization and electric polarization coexists, allowing for control of the magnetic field via applied voltage and electric field control via applied current density [1]. This is facilitated by the strain that arises between the magnetic and piezoelectric materials. Strong magnetoelectric coupling also allows for creation of more efficient, lightweight, and compact systems as compared to traditional materials. Notably, a heterostructure consisting of piezoelectric and ferromagnetic materials bonded together with adhesive to increase magnetoelectric coupling via strain. This allows for a new class of low-frequency, compact antennas of much smaller size as compared to traditional antennas operating at the same frequency [2].

The most common multiferroic architecture is a stacked magnetoelectric laminate with a piezoelectric material sandwiched between two magnetic materials. For transmitter applications, the piezoelectric layer is driven by an alternating voltage at its resonance frequency to generate strain in the piezoelectric material. The strain is transferred to the magnetic material, resulting in a change in magnetization and the emission of an oscillating magnetic field. The concept is schematically shown in Fig. 1(b), and referred to as Converse Magnetoelectric (CME) Effect. For receiver applications, an incident magnetic field produces an alternating voltage across the piezoelectric layer. This is schematically shown in Fig. 1(a), referred to as Direct Magnetoelectric (DME) Effect.

Magnetoelectric method of wireless power transfer has notably two main advantages [3]. The first one is its inherent advantages of miniaturization [4]. The second comes from the fact that low frequency has high penetration depth in tissues with low absorption [5]. Notably, ME systems usually do not operate at standard frequencies assigned to the wireless medical telemetry system [6]. Specifically, the resonant frequency fundamentally depends on the length of the layers. Higher length structures operate or resonate at lower frequency [7]. This research seeks to develop and demonstrate flexible multiferroic structures and their

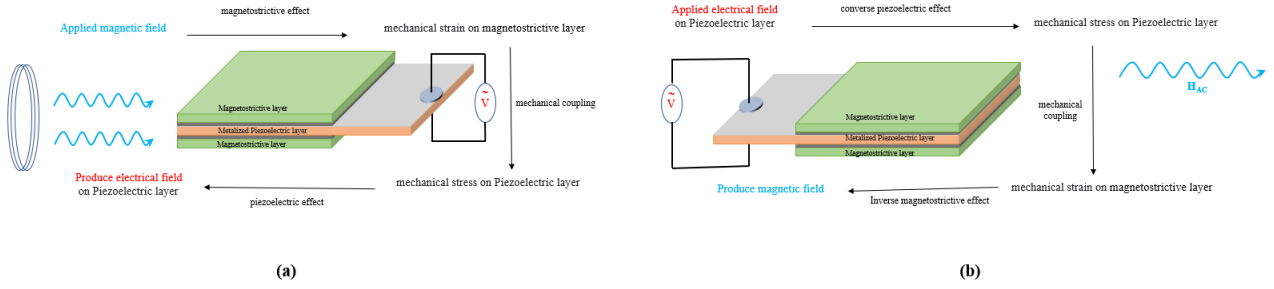


Fig. 1. Magnetoelectric (ME) Effect (a) Direct Magnetoelectric (DME) Effect (b) Converse Magnetoelectric (CME) Effect

integration with other power components to advance miniaturized power telemetry modules.

II. MATERIALS AND FABRICATION

Two different ME heterostructures (Fig. 2) that use varying magnetic fields at low frequency are examined to transfer power wirelessly. In both bimorph laminates, the magnetostrictive material was a 23- μm thick Magnetostrictive foil® 2605SA1 (Magnetostrictive foil® Inc., Conway, SC, USA). For the piezoelectric layers, macro fiber composite (MFC, M4010-P1) transducer (Smart Material Corp.) and flexible sheets of PVDF (polyvinylidene fluoride) (piezopvdf.com, PA, USA) were used in two different multiferroic structures. MFC (M4010-P1) is an aligned rectangular sheet of PZT piezo-fibers encapsulated in polyimide. Interdigitated electrodes are patterned on the latter. The dimensions of MFC are 40 mm \times 10 mm \times 350 μm .

Among the different thicknesses of PVDF material that are commercially available, 200 μm was chosen as it matches that of MFC. To create the resonator, sheets of Magnetostrictive foil® were cut into 40 mm \times 10 mm layers. Similarly, PVDF sheets were cut such that it could tightly accommodate the magnetostrictive layers. Finally, the bimorph laminate structures were fabricated by bonding two magnetostrictive layers on both sides of a single piezoelectric layer with an epoxy (WEST SYSTEM® 105 Epoxy Resin and hardeners) that was left overnight to be cured at room temperature.

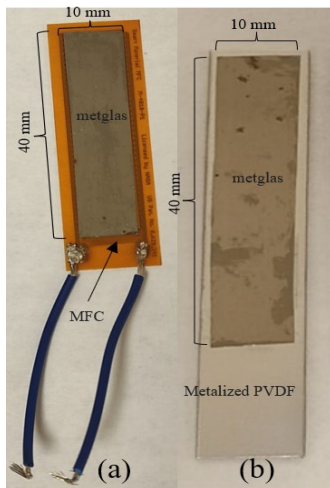


Fig. 2. ME samples, (a)MFC-Magnetostrictive foil, (b)PVDF-Magnetostrictive foil

Based on the combinations of poling orientation, we identified four different coupling modes (L-T, T-T, L-L and T-L) [8]. We specifically chose the L-T mode to resonate the PVDF-Magnetostrictive foil® test structures (Fig. 3). The magnetostrictive layer is longitudinally magnetized whereas PVDF is polarized along the direction of thickness and has a piezoelectric coefficient of d_{31} , $p > 25$ pC/N and d_{33} , $p = 26$ pC/N. Notably, MFC-P1 utilizes the longitudinal effect (d_{33} operational mode) and has a piezoelectric coefficient of d_{33} , $p = 460$ pC/N.

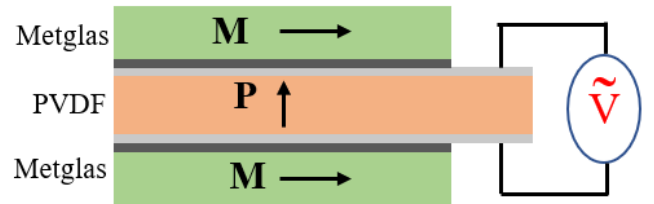


Fig. 3. L-T mode of PVDF-Magnetostrictive foil bimorph

III. ELECTRICAL CHARACTERIZATION

ME transducers are generally driven with varying magnetic field and biased with a static magnetic field. A Helmholtz two-coil setup was constructed to generate these field patterns. Fig. 4 shows the testing methodology. The outer Helmholtz coil was setup to deliver DC magnetic fields. This was connected to DC current source and worked as an electromagnet. The static field, which is proportional to the current in the coil, was easily controlled and measured using the 3-Axis wireless Magnetic Field Sensor (PS-3221, Pasco Scientific, USA). For the inner AC Helmholtz coil setup, AFG31022 Tektronix Function Generator (Tektronix Inc., Beaverton, USA) was used to produce the AC field. Since, the AC coil was not tuned with resonating capacitors, the coil impedance increased with AC frequency. This led to the attenuation of the amplitude of AC fields. In order to compensate for this, the coil was further connected to a AC waveform amplifier (Accel Instruments TS250). Using MC162 AC magnetic field sensor (Magnetic Sciences Inc., MA, USA), we were able to keep the AC field stable as we vary the frequency.

The equivalent circuit of a power generator is shown in Fig. 5, where CP represents the capacitance of piezoelectric layer, CF represents capacitance of filter and RL represents the load resistance. The rectification of the AC signal was

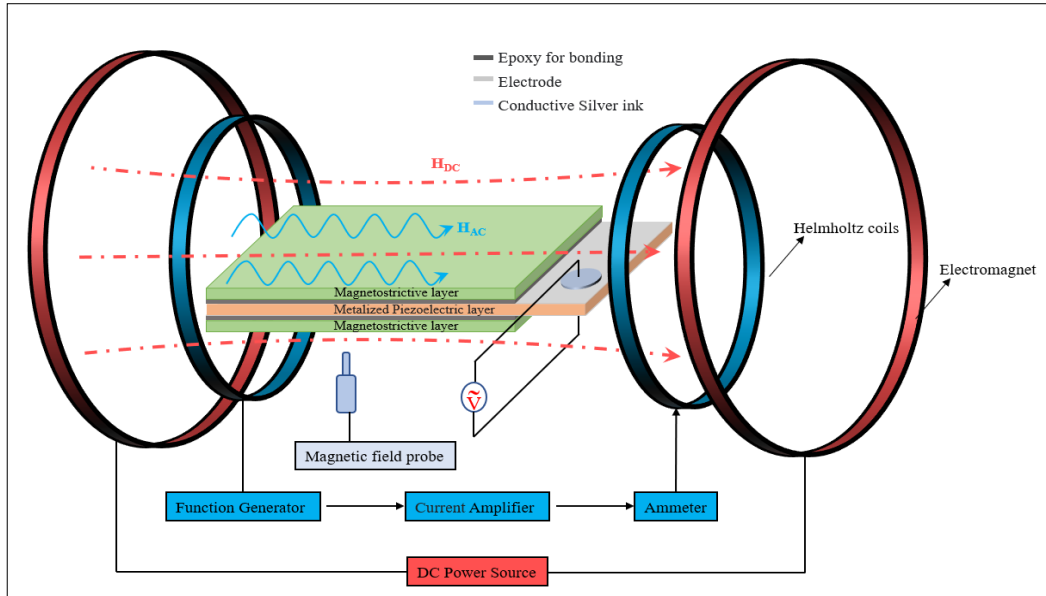


Fig. 4. Illustration of the magnetolectric experiment setup

achieved with a bridge rectifier and excess ripple was stabilized with a 10- μ F filter capacitor. The open circuit voltage was measured with Keysight Oscilloscope (MSOS254A). The output power was calculated using the formula, $P=VR^2/RL$, where VR is the rectified DC voltage. ME coefficient α_{ME} of PVDF-Magnetostrictive foil was calculated using the following formula: $\alpha_{ME} = V_{out} / (H_{AC} * t)$, where V_{out} output voltage, H_{AC} is input AC field strength and t is the thickness of piezoelectric layer [9].

It was found that the 12-Oe DC field was the optimum bias condition in this case. Under constant optimum DC field, the open circuit voltage has a linear relationship with the AC field strength. This relationship is expressed through the equation: $V_{out} = H_{ac} * \alpha_{ME} * t$ [10].

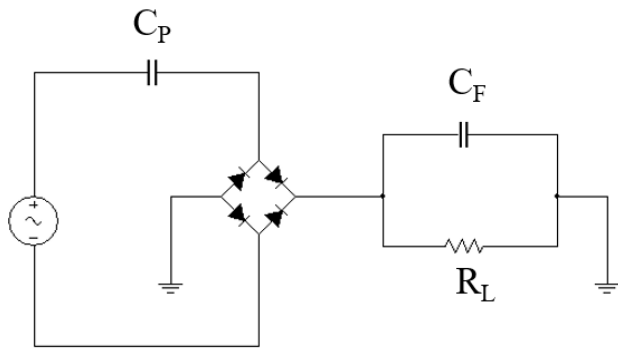


Fig. 5. Equivalent circuit of the power generator

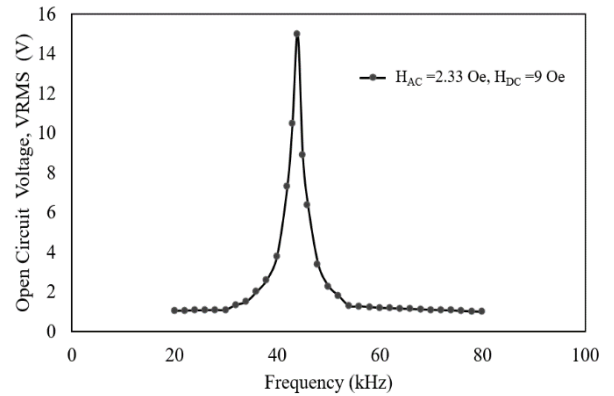


Fig. 6. Open Circuit Voltage of MFC-Magnetostrictive foil@ at various frequencies.

IV. RESULTS AND DISCUSSION

A. Characterization of multiferroic samples

The measured open circuit voltage of MFC-Magnetostrictive foil@ as a function of frequency is shown in Fig. 6. MFC-Magnetostrictive foil@ test structures resonated with a 15 Volts V_{RMS} at 44 kHz. As can be seen in Fig. 7, the open circuit voltage of MFC-Magnetostrictive foil is measured at two different AC magnetic fields (0.3 Oe and 3.4 Oe) across different frequencies, while keeping the DC field constant at 12 Oe. Notably, the resonant frequency didn't change with the varying amplitude of the incoming AC field.

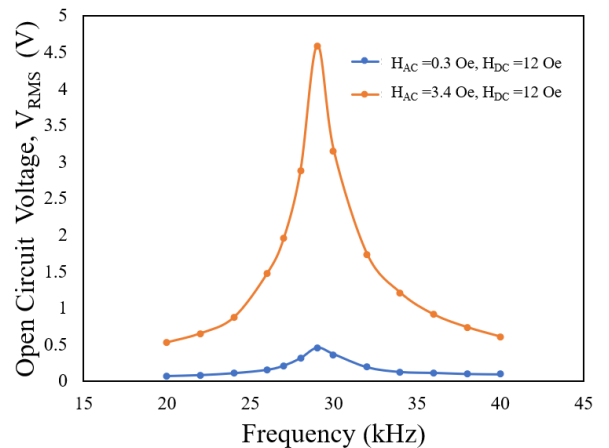


Fig. 7. Open Circuit Voltage of PVDF-Magnetostrictive foil® as a function of frequency.

Of course, the magnetostrictive layer has nonlinear characteristics [11], [12]. Due to this, a static magnetic field is applied to ensure that the AC field operates at the most sensitive point of the field-strain curve of the magnetostrictive material and produce significant mechanical strain in the magnetostrictive material [13]. This phenomenon can be illustrated in Fig. 8, where the ME coefficient α_{ME} reaches a maximum value that decreases gradually with more DC bias at a constant AC field.

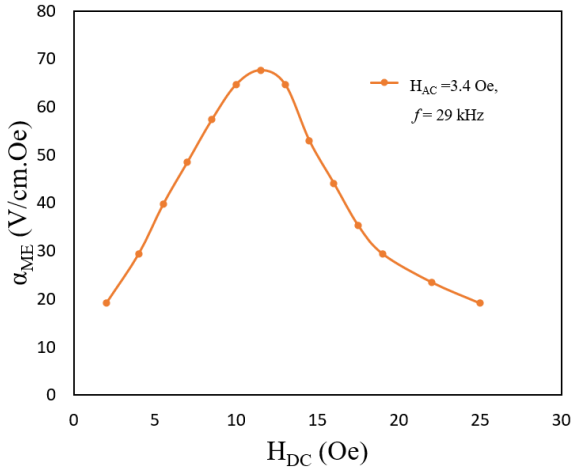


Fig. 8. ME coefficient α_{ME} of the PVDF-Magnetostrictive foil as a function of static bias magnetic field

The output power of the transducers was characterized further. Specifically, Figures 9 and 10 show the measured power output for the MFC-Magnetostrictive foil® and PVDF-Magnetostrictive foil®, respectively at different load resistances. In both figures, the output voltage increases with higher load resistance, whereas the output power increase drastically followed by a gradual decrease. Fig. 11 shows the optimum power output of PVDF-Magnetostrictive foil® at the resonant frequency. The DC field and the load resistance were optimized for the curves in Fig. 11.

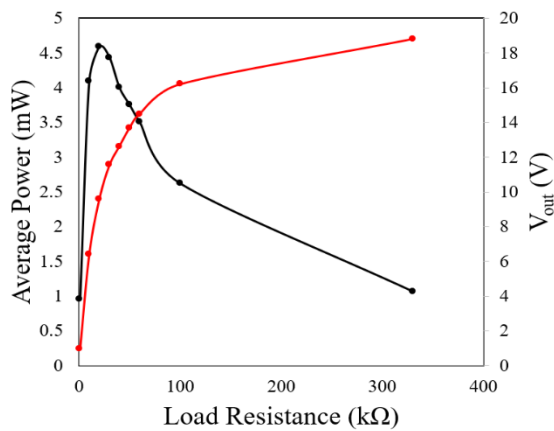


Fig. 9. Output power and output voltage of MFC-Magnetostrictive foil at different load resistances.

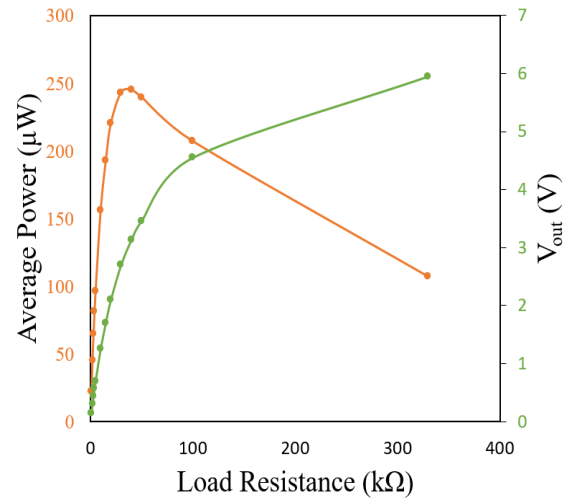


Fig. 10. Output power and output voltage of PVDF-Magnetostrictive foil® at different load resistances.

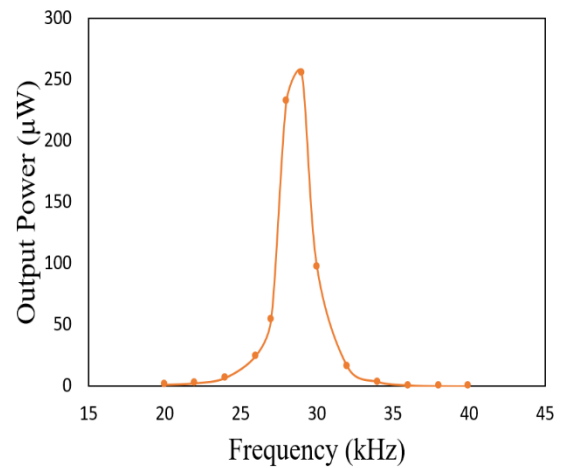


Fig. 11. Output power of the PVDF-Magnetostrictive foil across different frequencies with a 40 k Ω load resistance.

B. Package integration for multiferroic power telemetry

The AC voltage generated across the piezoelectric layer was further rectified using full-wave rectifier circuit on the LCP substrate. The desired copper traces for the circuitry was patterned using lithography and subtractive copper patterning techniques. Fig. 12 shows the schematic of the package integration for multiferroic power telemetry. Four different schottky diodes (Fig. 13a, 13b) were soldered to form a full-wave bridge rectifier. In Fig. 13c, two diode arrays were used in the same circuitry architecture as shown above. The filter capacitors were also connected in parallel with load resistance that smoothed the generated ripples. The ME system was assembled with the integrated circuitry to demonstrate a fully functioning multiferroic power telemetry (Fig. 14).

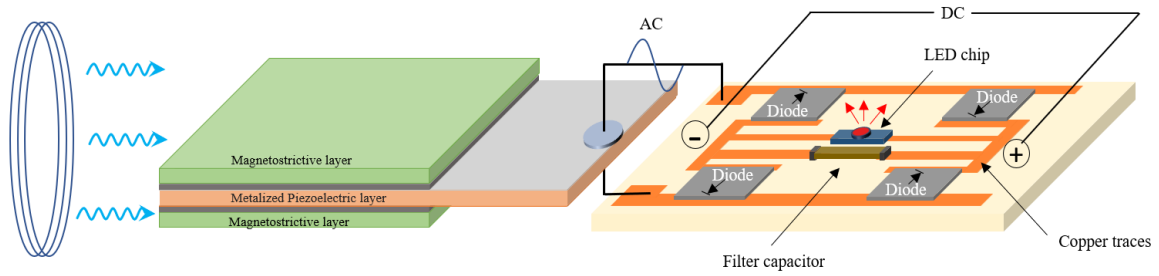


Fig. 12. Illustration of package integration for multiferroic power telemetry

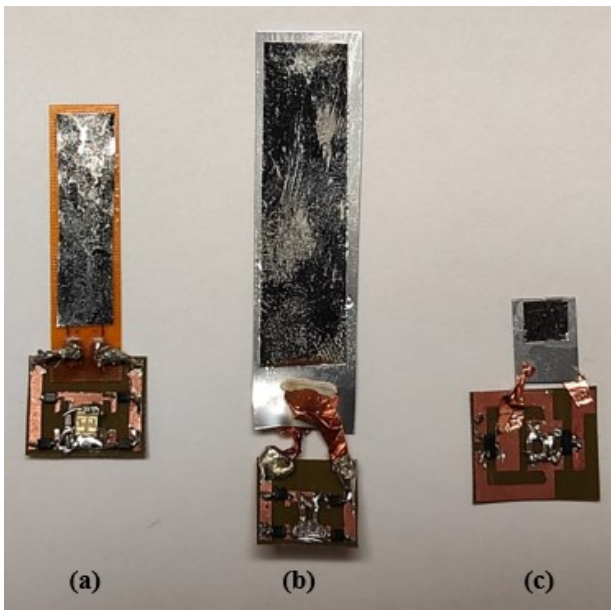


Fig. 13. Various ME bimorphs with integrated circuitry for power telemetry. (a) MFC-Magnetostrictive foil® (75 mm²), (b) PVDF-Magnetostrictive foil® (400 mm²), (c) PVDF-Magnetostrictive foil® (25 mm²)

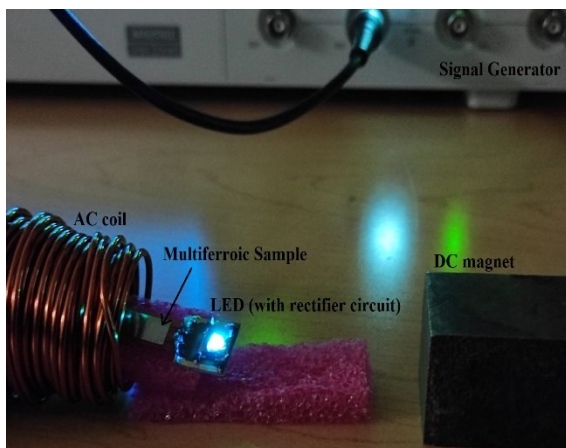


Fig. 14. Lighting of LED load with the fabricated ME bimorphs through power telemetry.

V. CONCLUSION

Multiferroic stacks of various compositions were fabricated with incorporated magnetostrictive alloys and piezoelectric polymer films. Thin epoxy adhesives were used to achieve the strain coupling. Using an optimized set up, the maximum power of ~4.6 mW was attained with the test-structures. By designing the antennas to resonate at 29 kHz, higher power densities can be achieved as stronger magnetic fields can be safely used. The flexible multiferroic structures can then be co-packaged with diodes and storage capacitor components to realize integrated power modules.

ACKNOWLEDGMENT

This research was financially supported by National Science Foundation (NSF), Grant number: 2029007 through its EARly-Concept Grants for Exploratory Research (EAGER) in Secure Analog-RF Electronics and Electromagnetics (SARE).

REFERENCES

- [1] Y. Wang, J. Hu, Y. Lin, and C.-W. Nan, "Multiferroic magnetoelectric composite nanostructures," *NPG Asia Mater*, vol. 2, no. 2, pp. 61–68, Apr. 2010, doi: 10.1038/asiamat.2010.32.
- [2] P. Gaire, V. Jaiswal, S. Y. B. Sayeed, J. L. Volakis, M. R. Pulugurtha, and S. Bhardwaj, "Tunable Multiferroics for Reconfigurable RF System Packages," in *2021 IEEE 16th Nanotechnology Materials and Devices Conference (NMDC)*, Dec. 2021, pp. 1–4. doi: 10.1109/NMDC50713.2021.9677517.
- [3] A. Singer and J. T. Robinson, "Wireless Power Delivery Techniques for Miniature Implantable Bioelectronics," *Adv Healthc Mater*, vol. 10, no. 17, p. 2100664, Sep. 2021, doi: 10.1002/adhm.202100664.
- [4] H. Lin *et al.*, "Future Antenna Miniaturization Mechanism: Magnetoelectric Antennas," in *2018 IEEE/MTT-S International Microwave Symposium - IMS*, Jun. 2018, pp. 220–223. doi: 10.1109/MWSYM.2018.8439678.

- [5] S. Kopyl, R. Surmenev, M. Surmeneva, Y. Fetisov, and A. Kholkin, "Magnetoelectric effect: principles and applications in biology and medicine—a review," *Mater Today Bio*, vol. 12, p. 100149, Sep. 2021, doi: 10.1016/j.mtbio.2021.100149.
- [6] A. Singer *et al.*, "Magnetoelectric Materials for Miniature, Wireless Neural Stimulation at Therapeutic Frequencies," *Neuron*, vol. 107, no. 4, pp. 631-643.e5, Aug. 2020, doi: 10.1016/j.neuron.2020.05.019.
- [7] L. Y. Fetisov *et al.*, "Nonlinear converse magnetoelectric effects in a ferromagnetic-piezoelectric bilayer," *Appl Phys Lett*, vol. 113, no. 21, p. 212903, Nov. 2018, doi: 10.1063/1.5054584.
- [8] T. Rupp, B. D. Truong, S. Williams, and S. Roundy, "Magnetoelectric Transducer Designs for Use as Wireless Power Receivers in Wearable and Implantable Applications," *Materials*, vol. 12, no. 3, p. 512, Feb. 2019, doi: 10.3390/ma12030512.
- [9] H. Zhang *et al.*, "Evaluation of Magnetostrictive foil/polyvinylidene fluoride magnetoelectric bilayer composites for flexible in-plane resonant magnetic sensors," *J Phys D Appl Phys*, vol. 54, no. 9, p. 095003, Mar. 2021, doi: 10.1088/1361-6463/abc990.
- [10] M. Vopsaroiu, M. Stewart, T. Fry, M. Cain, and G. Srinivasan, "Tuning the Magneto-Electric Effect of Multiferroic Composites via Crystallographic Texture," *IEEE Trans Magn*, vol. 44, no. 11, pp. 3017–3020, Nov. 2008, doi: 10.1109/TMAG.2008.2001649.
- [11] D. A. Burdin, D. V. Chashin, N. A. Ekonomov, Y. K. Fetisov, and A. Stashkevich, "Nonlinear magnetoelectric effects in a composite ferromagnetic-piezoelectric structure under harmonic and noise magnetic pumping," *J Magn Magn Mater*, vol. 449, pp. 505–509, Mar. 2018, doi: 10.1016/j.jmmm.2017.10.096.
- [12] P. Gaire, J. L. Volakis, S. Bhardwaj, V. Jaiswal, and M. R. Pulgurtha, "Reconfigurable Antennas and FSS with Magnetically-Tunable Multiferroic Components," in *2022 IEEE 72nd Electronic Components and Technology Conference (ECTC)*, May 2022, pp. 109–115. doi: 10.1109/ECTC51906.2022.00027.
- [13] F. T. Alrashdan, J. C. Chen, A. Singer, B. W. Avants, K. Yang, and J. T. Robinson, "Wearable wireless power systems for 'ME-BIT' magnetoelectric-powered bio implants," *J Neural Eng*, vol. 18, no. 4, p. 045011, Aug. 2021, doi: 10.1088/1741-2552/ac1178.